Precision Indoor Three-Dimensional Visible Light Positioning Using Receiver Diversity and Multilayer Perceptron Neural Network

Abdulrahman A Mahmoud, Zahir Ahmad, Olivier C L Haas, Sujan Rajbhandari

***Abstract*—In recent times, several applications requiring highly accurate indoor positioning systems have been developed. Since global positioning system (GPS) is unavailable/less accurate in the indoor environment, alternative techniques such as visible light positioning (VLP) is considered. The VLP system benefits from wide availability of illumination infrastructure, energy efficiency and absence of electromagnetic interference. However, there is a limited number of studies on three dimensional (3-D) VLP and the effect of multipath propagation on the accuracy of the 3-D VLP. This paper proposes a supervised artificial neural network (ANN) to provide accurate 3-D VLP whilst considering multipath propagation using receiver diversity. The results show that the proposed system can accurately estimate the 3-D position with an average RMS error of 0.0198m and 0.021m for line-of-sight (LOS) and non-line-of-sight (nLOS) link respectively. For 2-D localisation, the average RMS errors are 0.0103m and 0.0133m, respectively.**

***Index Terms*—Visible light positioning, Indoor 3-D positioning, Artificial neural network, multipath propagation, receiver diversity**

I. INTRODUCTION

In recent years, there has been an increase in demand for location-based services (LBSs) for autonomous robot control, indoor and underground parking, shopping centres and health applications. Although global positioning system (GPS) is one of the successful means of tracking objects in outdoor environments, GPS signals suffer significant attenuation and multipath fading in an indoor environment which results in large errors [1]. There are several radio-frequency (RF) based indoor positioning techniques such as Wi-Fi, Bluetooth, Radio frequency identification (RFID) which find applications in the indoor environment but exhibit certain limitations. Conventionally, the localisation accuracy of an RF system is in the decimeter range, due to multipath propagation and interferences [2]. However, applications such as autonomous robot and drone require accuracy in the cm to mm range. In addition to conventional two-dimensional (2-D) positioning, some of these applications require three-dimensional (3-D) positioning. Visible light positioning (VLP) has been shown to offer the high accuracy required by these applications and hence has been an active research topic for indoor positioning [3]. The suitability of VLP lies in its precision, ubiquity and cost-effectiveness. VLP is also free from electromagnetic interference but may suffer from ambient light interference.

Most works on indoor VLP focused on 2-D localisation assuming a fixed receiver height which ignores the position error introduced by variation in the height [4], [5]. There is limited reported work on 3-D localisation using VLP. An accelerometer in combination with light-emitting diodes (LEDs) was studied in [6] for 3-D positioning. The aforementioned work required the received power to be measured twice at different receiver orientation and a smartphone accelerometer was used to determine the receiver's orientation. Such work relies on the accuracy of the accelerometer which is less reliable if the target device is affected by a significant amount of movement [7]. An angle of arrival (AOA) approach to 3-D VLP was investigated using aperture-based receiver in [8]. Using multiple positioning algorithms such as triangulation, maximum likelihood and AOA, their model yielded an average root mean square (RMS) error of 0.1m in a room of 5m$\times$5m$\times$ 2m. A hybrid indoor localisation method was proposed in [4] using AOA and received signal strength (RSS) with multiple optical receivers. Their study demonstrated that an RMS error of less than 0.06m was achievable for a 2m$\times$ 2m$\times$ 2.5m room. However, their proposed system required information on the angles of the receiver prior to positioning. In [9], a 3-D VLP was proposed based on fingerprinting using K-means and random forest. However, the process of using fingerprinting technique is considered labour intensive and time consuming with respect to the size of the room. A recent study in [10] considered the use of receiver tilt to establish a 3-D VLP using RSS. Using receiver tilt, their mathematical model analysis shows an RMS error of 0.0795m in a 2.5m$\times$ 2.5m$\times$ 3m room. Note that most of the aforementioned studies did not consider the effect of reflection on the accuracy of the positioning. A recent study in [11] considered the effect of non-line-of-sight (nLOS) link to VLP using geometric relationship. The simulated and experimental results demonstrated that the positioning error increased linearly with respect to the reflection coefficient of the walls. In a room of 6m $\times$ 6m $\times$ 3m, their model yielded RMS errors up to 0.06843m. To achieve this accuracy, the coordinates of the LEDs were made irregular which is done to avoid having a symmetric matrix.

This work is supported by Petroleum Technology Development Fund (PTDF).

A. Mahmoud and O. Haas are with the Research Institute for Future Transport and Cities, Coventry University, Coventry CV1 5FB, U.K. (email: mahmou14@uni.coventry.ac.uk; csx259@coventry.ac.uk).

Z. Ahmad is with School of Computing, Electronics and Mathematics, Coventry University, Coventry CV1 2JH, UK. (email: ab7175@coventry.ac.uk).

S. Rajbhandari is currently with Huawei Technologies Sweden AB, Göteborg, Sweden. (email: sujan@ieee.org).

This, in turn, limits its practicality for real-life applications.

The adaptability and self-learning capability of artificial intelligence (AI) has recently led to the development of a number of 2-D and 3-D positioning applications using AI. For example, high-precision 2D VLP using deep neural network (DNN) based on Bayesian regularization with sparse training point was studied in [12]. A modified particle swarm optimisation (PSO) algorithm was used in [13] for 3-D positioning. However, only 605 points were tested in a room of 3m$\times$ 3m $\times$4m. Similarly, a modified genetic algorithm proposed in [14] required up to 76 iterations to provide optimal positioning. A high-precision 3-D positioning using artificial neural network (ANN) was studied in [5]. Their work required a large transmitter and receiver array with 4×4 LEDs grid at the ceiling with 1m spacing and a 19×19 receiver grid. Three ANNs (one for each dimension), each with 16 nodes in the input layer and 19 nodes in the output layer were required to determine the 3-D position. This made the approach complex as well as impractical due to the large ANN structure and the requirement for a large number of transmitters and receivers arrays. A recent study in [15] demonstrated the feasibility of 3-D VLP using a two-layer ANN. It was assumed that the room was divided into multiple trilateral positioning cells and only considered receivers below 0.8m in a room with a ceiling height of 2.7m hence only containing 30% of the room. Furthermore, the effect of multipath propagation was not considered in their study.

Hence, in this work, we propose a highly accurate 3-D VLP using the existing illumination infrastructure that is commonly available in a typical home/office/industrial environment. We also study the effect of multipath reflection on 3-D positioning and demonstrated that receiver diversity (i.e. multiple receivers each at different position) with ANN is very effective in providing accurate 3-D localisation with average room mean square (RMS) error of 0.021m for a typical room. To the best of the authors knowledge, this is the first study of 3-D indoor VLP combining receiver diversity with ANN to overcome the effect of multipath reflection.

The rest of this paper is structured as follows; the system description is provided in Section II. Section III describes the proposed application of supervised feed-forward back propagation multi-layer perceptrons (MLP) for 3-D localisation. The performance of the proposed system is discussed in Section IV. Finally, conclusions are drawn in Section V.

II. SYSTEM DESCRIPTION

This section describes the modelling of the VLP system and the factors that affect the reliability and accuracy of 3-D VLP. A typical indoor room with M (where $M > 1$) LED luminaries and $N \geq 1$ photodiodes (PD) based receiver proposed for this study is shown in Fig. 1. The transmitters transmit time division multiplex (TDM) or frequency division multiplex (FDM) signals encoded with their unique position information as outlined in [16].

The VLP in this study is based on received signal strength (RSS), which requires the estimation of the received power

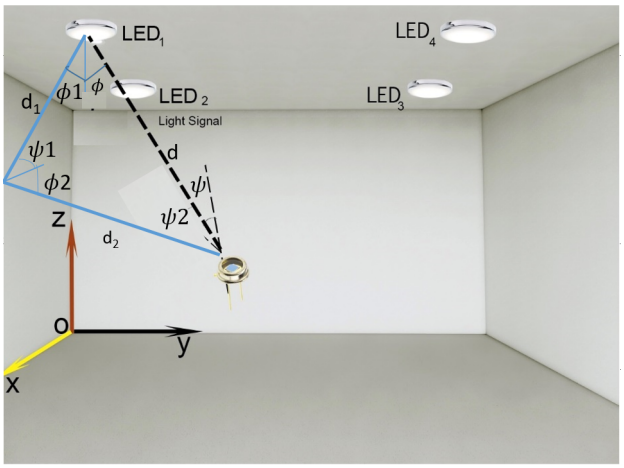

Fig. 1: Indoor localisation model for VLP

from various transmitter. For a typical room with both LOS and nLOS propagation paths, the received power $P_{r,i}$ from the i^{th} transmitter to the r^{th} receiver at the given location is given by:

$$P_{r,i} = (H_{los}(0) + H_{nlos}(0))P_{t,i} \tag{1}$$

where $P_{t,i}$ is the transmitted optical power from the i^{th} LED, $H_{los}(0)$ and $H_{nlos}(0)$ are the line-of-sight (LOS) and nLOS channel DC gain between the i^{th} LED and the r^{th} receiver, respectively.

The DC channel gain depends on the link distance, the channel configuration and the angle of incidence. For a LOS link with Lambertian radiation pattern, the DC channel gain is given by [17]:

$$H_{los}(0) = \begin{cases} \frac{(m+1)A_r}{2\pi d^2}\cos^m(\phi)T_s(\phi)g(\psi) \\ \cos(\psi) \qquad 0 \leq \psi \leq \Psi_c \\ 0, \qquad \psi > \Psi_c \end{cases} \tag{2}$$

where m is the Lambertian emission order, A_r is the PDs physical area, ϕ is the irradiance angle $T_s(\psi)$ is the optical filter gain, ψ is the angle of incidence, $g(\psi)$ is the optical concentrator gain, d is the distance between the receiver and the transmitter, Ψ_c is the PDs field of view. The Lambertian emission order and optical concentrator gain is given by:

$$m = \frac{-\ln 2}{\ln(\cos\phi_{1/2})}, g(\psi_i) = \frac{n_c^2}{\sin^2\psi} \tag{3}$$

where $\phi_{1/2}$ represents the half-power angle of the LED, n_c is the concentrator's refractive index. Under the assumption that the walls are composed of several reflectors ΔA and a reflection coefficient of ρ, the nLOS channel model is given by:

$$H_{nlos}(0) = \begin{cases} \sum_{\text{wall}} \frac{(m+1)A_r\rho\Delta A}{2\pi^2 d_1^2 d_2^2}\cos^m(\phi_1)\cos(\psi_1)\cos(\phi_2) \\ \cos(\psi_2)T_s(\phi_2)g(\psi_2) \qquad 0 \leq \psi_2 \leq \Psi_c \\ 0, \qquad \psi_2 > \Psi_c \end{cases} \tag{4}$$

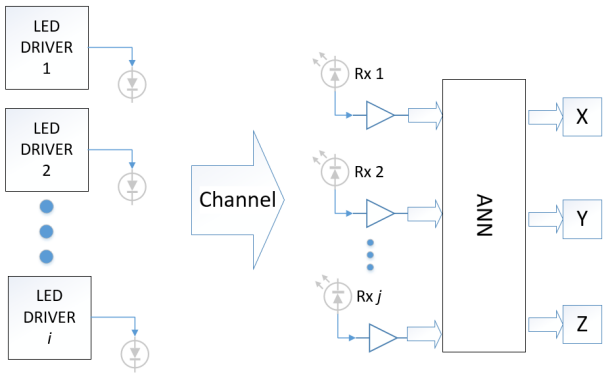

Fig. 2: Schematic of proposed VLP using ANN

where ψ_1 and ψ_2 are the angles of incidence, d_1 and d_2 are the distances, and ϕ_1 and ϕ_2 are angles of irradiance.

The accuracy of VLP is also affected by the additive white Gaussian noise (AWGN). The AWGN noise in the VLP system consists of thermal and shot noises. The noise generated by the background light and the desired optical signal is known as shot noise and its variance is given by:

$$\sigma^2_{shot,i} = 2qI_{bg}I_2B + 2qR_pP_{r,i}B \tag{5}$$

where B represents the bandwidth, R_p is the responsivity of the PD, I_2 is a noise bandwidth factor of the current, I_{bg} is the background current and q is the electronic charge. The thermal noise that arises from the amplifier at the receiver is given as:

$$\sigma^2_{thermal} = \frac{8\pi kT_k}{G}\eta AI_2B^2 + \frac{16\pi^2kT_k\Gamma}{g_m}\eta^2A^2I_3B^3 \tag{6}$$

where k represents the Boltzmann's constant. η, G and T_k represent the fixed capacitance of the PD, the open-loop gain and the absolute temperature respectively. I_3 is the noise bandwidth factor. g_m and Γ represent FET trans-conductance and FET channel noise factor, respectively.

III. Three dimensional localisation based on Artificial Neural Network

This section describes the proposed supervised feed-forward back propagation MLP ANN for 3-D localisation as shown in Fig. 2. TDM or FDM are assumed to be applied at the transmitter to be able to differentiate signals from individual transmitters. The received signal from the transmitters (in our case, four transmitters) at various receivers given by (1) are first de-multiplexed and then fed to an ANN.

We consider a MLP ANN with an input layer, hidden layer(s) and output layers. The number of neurons in the input layer is equal to the number of received signals from the transmitters to the receivers (i.e. $M \times N$). The output layer has three neurons corresponding to the three coordinates that are required to be estimated. Log-sigmoid is used as the activation function for the hidden layers and linear transfer function for the output layer. The ANN is first trained by selecting 1000 random 3-D location within the room. A feed-forward back-propagation method is initiated with the received signal as an input vector. Levenberg-Marquardt back-propagation is used as the training function which updates the weights and bias values over 100 epochs. The details of the ANN structure and training algorithm can be found in [18].

TABLE I: Simulation parameters for the ANN-based localisation

Parameter	Value
Room parameters [L × W× H] (m)	$5 \times 5 \times 5$
Number of transmitters (M)	4
Transmitter power (W)	10
Transmitter semi-angle (degree)	60
No of receiver (N)	$[1, 4]$
Receiver area, A (cm^3)	1
Optical filter gain	1
Receiver separation (m)	$[0.02, 0.2]$
Noise bandwidth, B (Hz)	0.6
Noise bandwidth factor (I_2)	0.562
FET channel noise factor Γ	1.5
Fixed capacitance of PD (pF/cm^2)	112
Temperature (T_k) (K)	295
FET transconductance (mS)	30
Background current $(I_{bg})\mu$ A)	740
Noise bandwidth factor (I_3)	0.0868

Finally, the proposed system is also evaluated for 2D VLP assuming a receiver at the height of 0m. At first, the ANN is trained within 1000 random samples with the room to estimate the x and y co-ordinates of the receiver. Subsequently the algorithm was evaluated to apprehend the accuracy of the model, see Section IV. Note that the number of neurons in the output layer is two, corresponding to x and y co-ordinates required for 2-D localisation.

IV. Results and Discussion

In this section, we evaluate the performance of the proposed 3-D VLP in a typical room environment. The criteria adopted to evaluate the results include the RMS error across the room and the cumulative distributive function (CDF) of the RMS error. The RMS error is defined as:

$$RMSerror = \sqrt{(x-\hat{x})^2 + (y-\hat{y})^2 + (z-\hat{z})^2} \tag{7}$$

where (x, y, z) is the real position and $(\hat{x}, \hat{y}, \hat{z})$ is the estimated position.

A 5m×5m×5m room with uniformly distributed four LED transmitters located at $(1.25, 1.25)$m, $(3.75, 1.25)$m, $(1.25, 3.75)$m and $(3.75, 1.25)$m on the ceiling is considered so that the illumination is uniform [17]. We considered 8 million random locations within the room with a height ranging from 0m up to 2.5m covering 50% of the rooms height. We also consider receiver diversity with $N = [1, 4]$, where all receivers point towards the ceiling. Additional parameters used for the simulation are shown in Table I.

A. Artificial Neural Network Tuning

In this subsection, we optimise the parameters of the MLP-ANN. Increasing the number of neurons tends to offer better performance at the cost, however, of higher complexity,

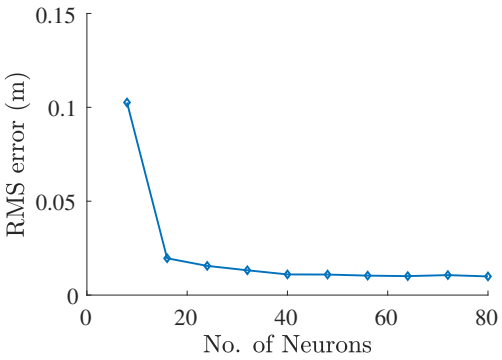

Fig. 3: Average RMS error of 3-D VLP as a function of the number of neurons in the hidden layer.

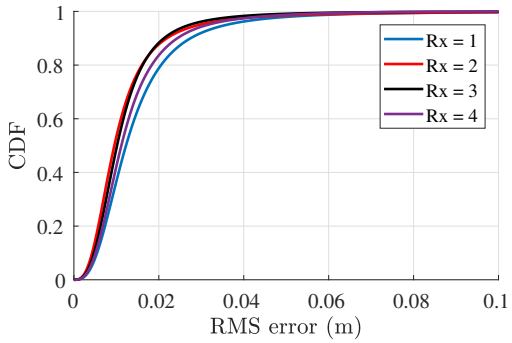

Fig. 4: RMS error versus the CDF for 3-D VLP with diversity order of $N = [1, 4]$ receivers for LOS link.

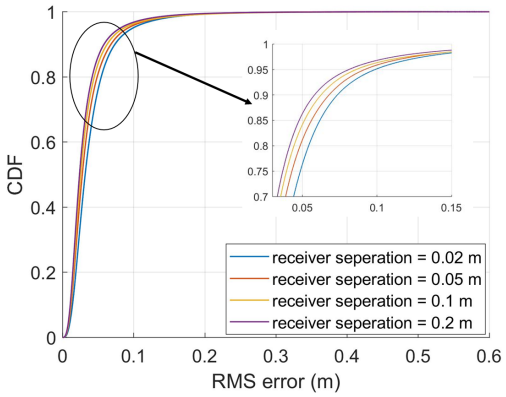

Fig. 5: RMS error versus the CDF for 3-D VLP with diversity order of two and different receiver separation distance.

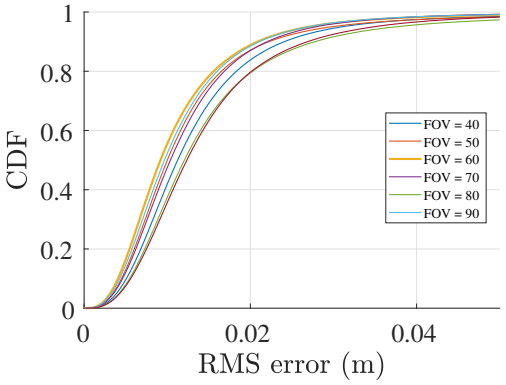

Fig. 6: CDF of 3D VLP as a function of receiver FOV.

larger training set, longer training time and higher memory requirement. Hence, it is necessary to optimise the ANN for optimum performance. The simulation shows that two hidden layers offer the optimum performance. In order to simplify the optimisation problem, the number of neurons in the hidden layers are made equal and is taken as a multiple of the diversity order (i.e. $M \times N$). We varied the number of neurons in the hidden layer from 8 to 80 (i.e. $10M \times N$), without changing the training length and other parameters, then estimated the RMS error for various number of neurons. Fig. 3 shows the RMS error as a function of the number of neurons in the hidden layers. The figure clearly demonstrates that increasing the number of neurons improves the performance. There is a sharp reduction in RMS error when the number of neurons in the hidden layer is increased from 8 to 16, then the slope reduces. Beyond 32, there is only a marginal improvement in the performance. Therefore, an MLP with 32 neurons in the hidden layers was adopted in the rest of the study as this provides the best trade-off between complexity and performance.

B. Results

Fig. 4 shows the RMS error versus CDF for 3-D VLP obtained using the proposed ANN with a diversity order of 1 to 4 for LOS link. The receivers are located in a rectangular grid with separation of 0.02m. This separation between the receivers is considered in order to make the receiver system as compact as possible. As demonstrated in Fig. 4, there is a significant improvement in VLP using receiver diversity. For example, the RMS error using a single receiver is 0.037m at 0.95 CDF. This value reduces to less than 0.033m when two or more receivers are used. Furthermore, increasing the number of receivers beyond two does not improve the performance significantly. For example, the RMS error values at 0.95 CDF (and average RMS errors) are $0.0312(0.0124)$m, $0.029(0.0122)$m and $0.0329(0.0136)$m for diversity order of $2, 3$ and 4, respectively. The diversity order of 4 results in higher errors due to the requirement of longer training length and larger ANN size for the optimum performance. Hence, we consider only two receivers in the rest of the studies as this provide the best trade-off between complexity, computational requirements and system performance.

The separation between the receiver elements also plays a critical role in VLP position (i.e. the distance between two receivers can also affect the positioning accuracy). We considered both practicality and functionality of the system. Hence, we optimise the separation between the receiver elements for the diversity order of two. We only consider the separation

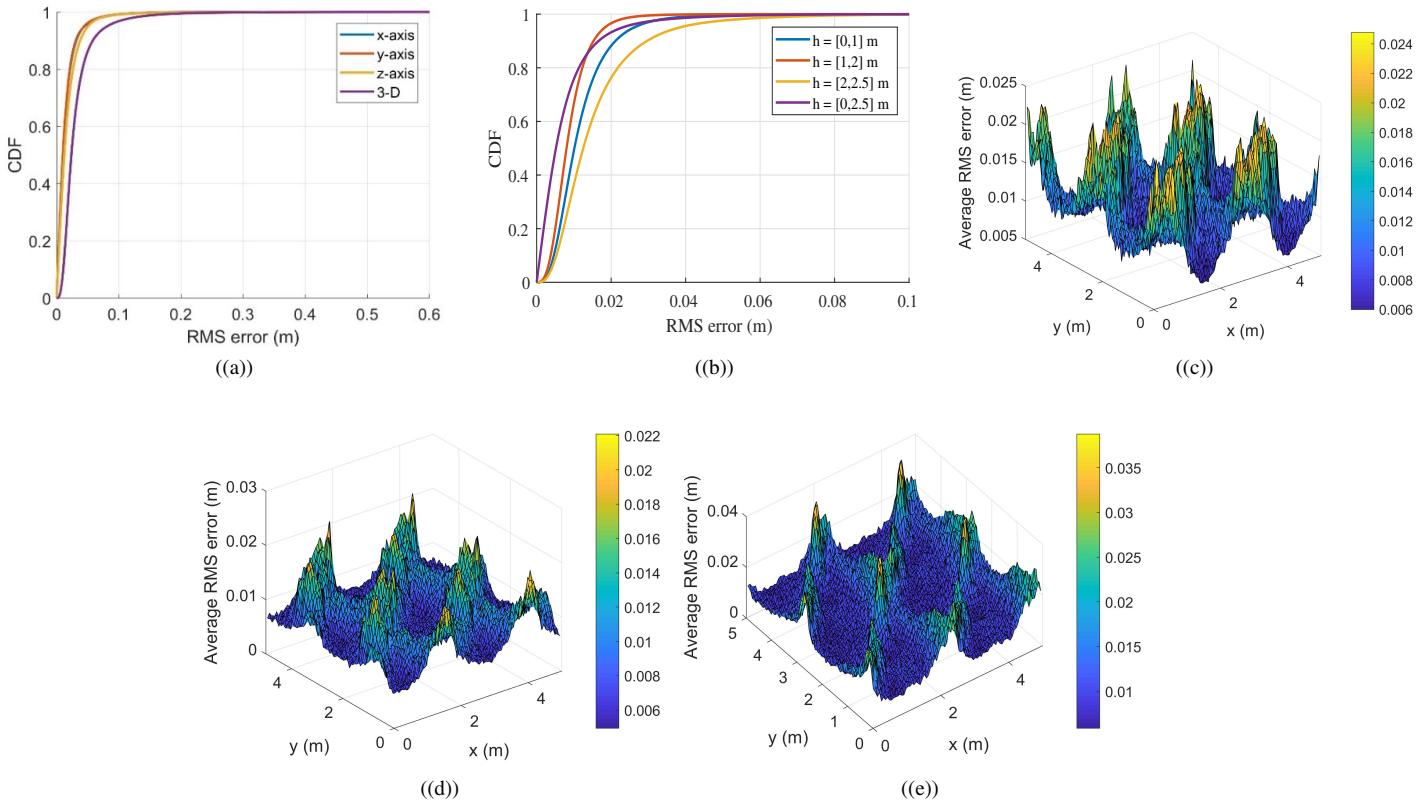

Fig. 7: CDF versus RMS error for 3D VLP using the optimum system parameters for a LOS link: a) error across the three different axes, b) error across various height c) average RMS distribution across the room averaged over the height of 0 m to 1 m d) average RMS distribution across the room averaged over the height of 1 m to 2 m and e) average RMS distribution across the room averaged over the height of 2 m to 2.5 m)

from 0.02m to 0.2m, as a receiver separation of less than 0.02m is not possible due to photodiode size and a separation beyond 0.2m would make the receiver separations too large for practical applications. Fig. 5 shows the positioning RMS error against the CDF for the various receiver separations. For example, at 0.95 CDF, the 3-D position accuracy improves from 0.034m to 0.033m when the receiver separation is increased from 0.02m to 0.05m, respectively. Increasing the receiver separation beyond 0.05m provides some improvements. This illustrates that increasing the receiver separation improves the accuracy of the model. The average RMS errors for the receiver separation of 0.02m, 0.05m, 0.1m and 0.2m are 0.012m, 0.012m, 0.013m and 0.015m, respectively. The error is seen to reduce with respect to increasing the receiver separation because the receivers take advantage of a very low probability of simultaneous dropouts with larger distances between them. Hence, in the following discussion, we will only consider the diversity receiver with separation of 0.2m.

The performance of 3D VLP also depends on the FOV of the receiver. Fig. 6 shows the CDF of 3-D VLP against the receiver FOV of 40° to 90°. In order to differentiate the performance improvement due to FOV from single strength gain (in increase in signal-to-noise ratio), the optical gain at

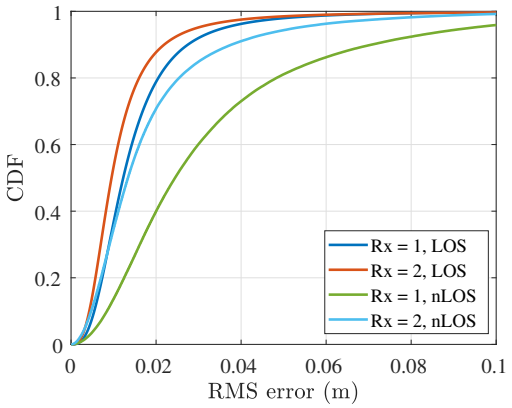

Fig. 8: CDF of 3D LOS vs non-LOS

all the FOVs are considered unity. Note that the optical gain and FOV are related and the maximum gain for a given FOV is governed by Etendue [19]. Fig. 6 shows that increasing the receivers FOV from 40° to 60° offers a significant improvement in performance. However, FOVs beyond 60° degrade the performance. Hence, in the rest of the paper, we selected a receiver FOV of 60° as this provides near the optimum

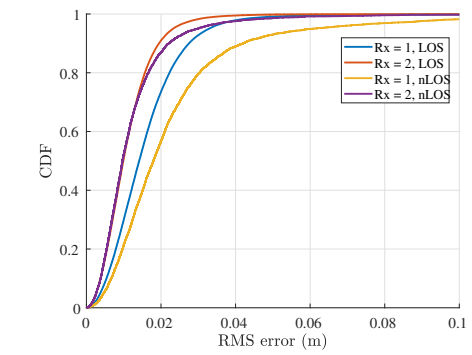

((a))

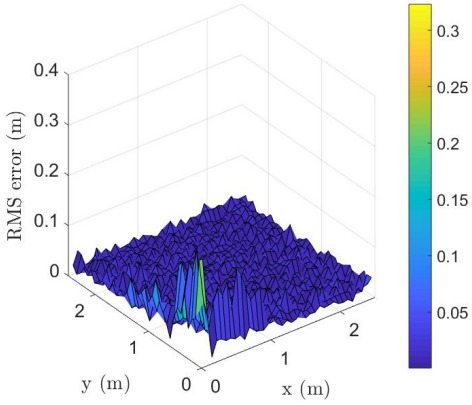

((b))

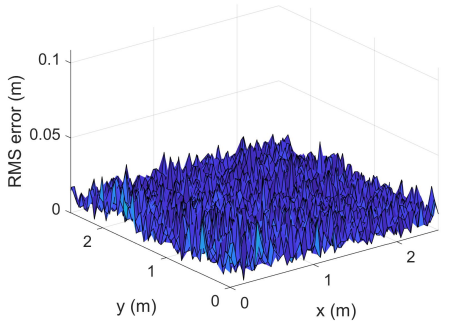

((c))

Fig. 9: CDF versus RMS error for 2D VLP using ANN and receiver diversity: a) CDF of RMS error for LOS and non-LOS link with 1 and 2 receivers. b) RMS error distribution for an nLOS link in a quarter of the room with 1 receiver and c) RMS error distribution for the nLOS link in a quarter of the room with 2 receivers.

performance.

Using the optimum parameters obtained for the 3-D VLP ANN, the performance of 3-D VLP using receiver diversity and ANN is simulated considering LOS link and results are shown in Fig. 7. Fig. 7(a) shows the contribution of errors in x, y and z-axis separately to the overall performance. As it can be seen from Fig. 7(a), each axis contributes almost equally to the overall error. Fig. 7(b) shows the CDF of the estimation error at various height range, separated into the region of $[0, 1]$m, $[1, 2]$m and $[2, 2.5]$m. Fig.7 (c) to (e) shows the average RMS error distributions across the room over the height of $[0, 1]$m, $[1, 2]$m and $[2, 2.5]$m. As can be seen from Fig. 7(b), the average error for the height of $[0, 1]$m and $[1, 2]$m are almost equal with the values of 0.0119m and 0.0091m. However, the position error in the range of 2 to 2.5m is higher than the height less than 2m with the average error of 0.0198m. Average RMS error distribution in Fig. 7 (c) and (d) shows that the proposed system can accurately estimate the 3D position across the room. There is an interesting pattern found in the error distribution. The highest position estimation error occurs across the diagonal where the signal strength from two transmitters to the receivers are identical. However, there is a higher estimation error at the edge of the room and the highest error occurs at the corner of the room. Throughout the room the estimation error is higher for heights above 2m than it is for height below 2m. At the height of 2m, due to the limited divergence angle of the LEDs and limited FOV of the receiver, the received signal strength from one or more LEDs is very weak leading to higher estimation error. In order to reduce the estimation error above this height, the number of transmitters needs to be increased.

As mentioned in the previous section, the multipath propagation also affects the position estimation especially close to the wall where the reflected signal strength is at the highest. We evaluate the performance of receiver diversity VLP considering a) LOS path only and b) LOS and nLOS propagation path for one and two receivers with the results presented in Fig. 8. Fig. 8 clearly shows that multipath propagation reduces the accuracy in the position estimation for a single receiver. The RMS error value at CDF of 0.95 increases from 0.037m for a LOS link to 0.094m for a nLOS, using a single receiver. However, diversity receiver significantly improves the performance for both LOS and nLOS link with an RMS error of 0.0198m and 0.021m, respectively.

The CDF of the RMS error for 2D VLP considering the LOS and non-LOS link using receiver diversity and ANN and receiver diversity is shown in Fig. 9(a). There is a reduction in performance between LOS and nLOS link for a single receiver with RMS error values of 0.033m and 0.066m respectively at CDF of 0.95. The average errors for LOS and nLOS links with two receivers are 0.0103m and 0.0133m, respectively. The RMS error distributions in Fig. 9(b) and (c) shows that receiver diversity reduces error close to the walls yielding to a lower average and RMS errors.

We performed a comparative study of the proposed technique with other states of the art 3-D-VLP techniques and summarised the results in Table II. Note that some of the work in the literature considered small room dimension (e.g. [9], [15]), which tends to improve the accuracy. Though the best performance is achieved in [5], this is largely impractical due to the requirement for a large number of transmitters (16) and receivers (361). Most of the existing work does not include

TABLE II: Comparative study of the proposed system with published work.

Paper	Method	Channel model	Transmitter	Receiver	Room dimension(m)	RMS error (m)
[5]	Three ANN	LOS	4×4	19×19	$4 \times 4 \times 3$	0.0004
[8]	AOA	LOS	4	1	$5 \times 5 \times 2$	0.1
[9]	Fingerprinting	LOS	4	1	$2 \times 2 \times 5$	0.0445
[11]	Geometrical relationship	LOS+nLOS	4	1	$6 \times 6 \times 3$	0.06843
[14]	Genetic algorithm	LOS	4	1	$3 \times 3 \times 4$	0.021
[15]	2-layer ANN	LOS	4	1	$0.9 \times 1 \times 0.4$	0.009
[20]	Trilateration	LOS	4	1	$5 \times 5 \times 5$	0.091
[21]	Differential evolution algorithm	LOS	4	1	$4 \times 4 \times 3$	0.01
This work	ANN with receiver diversity	LOS+nLOS	4	2	$5 \times 5 \times 5$	0.021

nLOS link. However, as reported in [11], the inclusion of nLOS increases the RMS error up to 0.06843m. Therefore, whilst the work in [21] yielded an average RMS error of 0.01m, including nLOS link and a larger room volume would likely increase the stated error. By comparison, simulating the system using the identical condition to that presented in [21], results in average RMS error of 0.007m is compared to 0.01m in [21]. Based on these results, the proposed solution is not only practical but also offer the best 3-D positioning results among the algorithms that had been studied so far whilst accounting for LOS and nLOS.

V. CONCLUSIONS

In this paper, we proposed an indoor visible light localisation using receiver diversity with ANN. We have evaluated the performance of the proposed system in a typical room environment. For optimum performance, the ANN parameters and FOV were optimised. The study clearly shows that the receiver diversity significantly improves the 3-D localisation. The performance improvement is even more significant when multipath propagation is considered. The study shows that the receiver diversity with ANN can provide accurate 2-D positioning with an average RMS error of 0.0103m and 0.0133m for LOS and nLOS links, respectively. For the 3-D localisation, the average RMS errors are 0.0198m and 0.021m, respectively. Hence, in this study, we have demonstrated using simulation, the feasibility of precise localisation even in the link affected by multipath propagation using receiver diversity and neural network.

REFERENCES

[1] C. Sun, H. Zhao, W. Feng, and S. Du, "A frequency-domain multipath parameter estimation and mitigation method for BOC-modulated GNSS signals," *Sensors (Switzerland)*, vol. 18, no. 3, 3 2018.

[2] O. Popoola, S. Sinanović, W. Popoola, and R. Ramirez-Iniguez, "Optical Boundaries for LED-Based Indoor Positioning System," *Computation*, vol. 7, no. 1, pp. 1–7, 2019.

[3] T. H. Do and M. Yoo, "An in-depth survey of visible light communication based positioning systems," *Sensors (Switzerland)*, vol. 16, no. 5, 5 2016.

[4] S. H. Yang, H. S. Kim, Y. H. Son, and S. K. Han, "Three-dimensional visible light indoor localization using AOA and RSS with multiple optical receivers," *Journal of Lightwave Technology*, vol. 32, no. 14, pp. 2480–2485, 2014.

[5] I. Alonso-González, D. Sánchez-Rodríguez, C. Ley-Bosch, and M. A. Quintana-Suárez, "Discrete indoor three-dimensional localization system based on neural networks using visible light communication," *Sensors (Switzerland)*, vol. 18, p. 1040, 2018.

[6] M. Yasir, S. W. Ho, and B. N. Vellambi, "Indoor positioning system using visible light and accelerometer," *Journal of Lightwave Technology*, vol. 32, no. 19, pp. 3306–3316, 10 2014.

[7] D. P. Nicolella, L. Torres-Ronda, K. J. Saylor, and X. Schelling, "Validity and reliability of an accelerometer-based player tracking device," *PLoS ONE*, vol. 13, no. 2, 2018. [Online]. Available: https://doi.org/10.1371/journal.pone.0191823

[8] H. Steendam, "A 3-D Positioning Algorithm for AOA-Based VLP with an Aperture-Based Receiver," *IEEE Journal on Selected Areas in Communications*, vol. 36, no. 1, pp. 23–33, 1 2018.

[9] J. Jiang, W. Guan, Z. Chen, and Y. Chen, "Indoor high-precision three-dimensional positioning algorithm based on visible light communication and fingerprinting using K-means and random forest," *Optical Engineering*, vol. 58, no. 1, 2019.

[10] D. Kim, J. K. Park, and J. T. Kim, "Three-Dimensional VLC Positioning System Model and Method Considering Receiver Tilt," *IEEE Access*, vol. 7, pp. 132 205–132 216, 2019.

[11] J. Xu, H. Shen, W. Xu, H. Zhang, and X. You, "LED-Assisted Three-Dimensional Indoor Positioning for Multiphotodiode Device Interfered by Multipath Reflections," in *2017 IEEE 85th Vehicular Technology Conference (VTC Spring)*. Sydney, NSW, Australia: IEEE, 2017, pp. 1–6.

[12] H. Zhang, J. Cui, L. Feng, A. Yang, H. Lv, B. Lin, and H. Huang, "High-Precision Indoor Visible Light Positioning Using Deep Neural Network Based on the Bayesian Regularization with Sparse Training Point," *IEEE Photonics Journal*, vol. 11, no. 3, 6 2019.

[13] Y. Cai, W. Guan, Y. Wu, C. Xie, Y. Chen, and L. Fang, "Indoor high precision three-dimensional positioning system based on visible light communication using particle swarm optimization," *IEEE Photonics Journal*, vol. 9, no. 6, 12 2017.

[14] H. Chen, W. Guan, S. Li, and Y. Wu, "Indoor high precision three-dimensional positioning system based on visible light communication using modified genetic algorithm," *Optics Communications*, vol. 413, pp. 103–120, 4 2018.

[15] J. He, C.-W. Hsu, Q. Zhou, M. Tang, S. Fu, D. Liu, L. Deng, and G.-K. Chang, "Demonstration of high precision 3D indoor positioning system based on two-layer ANN machine learning technique," Tech. Rep., 2019.

[16] M. Z. Afgani, H. Haas, H. Elgala, and D. Knipp, "Visible light communication using OFDM," in *2nd International Conference on Testbeds and Research Infrastructures for the Development of Networks and Communities, TRIDENTCOM 2006*, vol. 2006, 2006, pp. 129–134.

[17] Z. Ghassemlooy, W. Popoola, and S. Rajbhandari, *Optical wireless communications: System and channel modelling with MATLAB®*. Florida USA: CRC Press, 2017.

[18] S. S. Haykin and S. S. Haykin, *Neural networks and learning machines*. Prentice Hall/Pearson, 2009.

[19] X. J. Yu, Y. L. Ho, L. Tan, H. C. Huang, and H. S. Kwok, "LED-based projection systems," *IEEE/OSA Journal of Display Technology*, vol. 3, no. 3, pp. 295–303, 9 2007.

[20] D. Plets, Y. Almadani, S. Bastiaens, M. Ijaz, L. Martens, and W. Joseph, "Efficient 3D trilateration algorithm for visible light positioning," *Journal of Optics (United Kingdom)*, vol. 21, no. 5, 2019.

[21] Y. Wu, X. Liu, W. Guan, B. Chen, X. Chen, and C. Xie, "High-speed 3D indoor localization system based on visible light communication using differential evolution algorithm," *Optics Communications*, vol. 424, pp. 177–189, 2018.